Atypical retinoids ST1926 and CD437 are S-phase-specific agents causing DNA double-strand breaks: significance for the cytotoxic and antiproliferative activity

Claudia Valli,[1] Gabriela Paroni,[1] Angela Maria Di Francesco,[4] Riccardo Riccardi,[4] Michele Tavecchio,[2] Eugenio Erba,[2] Andrea Boldetti,[1] Maurizio Gianni',[1] Maddalena Fratelli,[1] Claudio Pisano,[6] Lucio Merlini,[3] Antonio Antoccia,[5] Chiara Cenciarelli,[5] Mineko Terao,[1] and Enrico Garattini[1]

[1]Laboratory of Molecular Biology, Department of Biochemistry and Molecular Pharmacology, and [2]Flow Cytometry Unit, Department of Oncology, Istituto di Ricerche Farmacologiche ''Mario Negri'' Milano, Italy; [3]Dipartimento di Scienze Molecolari Agroalimentari, Università degli Studi di Milano, Milan, Italy; [4]Division of Pediatric Oncology, Catholic University of Rome; [5]Department of Biology, Università ''Roma Tre,'' Roma, Italy; and [6]Sigma-Tau Industrie Farmaceutiche Riunite SPA, Pomezia, Italy

Abstract

Retinoid-related molecules (RRM) are novel agents with tumor-selective cytotoxic/antiproliferative activity, a different mechanism of action from classic retinoids and no cross-resistance with other chemotherapeutics. ST1926 and CD437 are prototypic RRMs, with the former currently undergoing phase I clinical trials. We show here that ST1926, CD437, and active congeners cause DNA damage. Cellular and subcellular COMET assays, H2AX phosphorylation (γ-H2AX), and scoring of chromosome aberrations indicate that active RRMs produce DNA double-strand breaks (DSB) and chromosomal lesions in NB4, an acute myeloid leukemia (AML) cell line characterized by high sensitivity to RRMs. There is a direct quantitative correlation between the levels of DSBs and the cytotoxic/antiproliferative effects induced by RRMs. NB4.437r blasts, which are selectively resistant to RRMs, do not show any sign of DNA damage after treatment with ST1926, CD437, and analogues. DNA damage is the major mechanism underlying the antileukemic activity of RRMs in NB4 and other AML cell lines. In accordance with the S-phase specificity of the cytotoxic and antiproliferative responses of AML cells to RRMs, increases in DSBs are maximal during the S phase of the cell cycle. Induction of DSBs precedes inhibition of DNA replication and is associated with rapid activation of ataxia telangectasia mutated, ataxia telangectasia RAD3-related, and DNA-dependent protein kinases with subsequent stimulation of the p38 mitogen-activated protein kinase. Inhibition of ataxia telangectasia mutated and DNA-dependent protein kinases reduces phosphorylation of H2AX. Cells defective for homologous recombination are particularly sensitive to ST1926, indicating that this process is important for the protection of cells from the RRM-dependent DNA damage and cytotoxicity. [Mol Cancer Ther 2008;7(9):2941–54]

Introduction

Retinoid-related molecules (RRM) are selective antitumor agents with no-cross resistance with other chemotherapeutics (1). CD437 is the prototypical RRM, whereas ST1926 is the most powerful and least toxic compound (2, 3). ST1926 is undergoing phase I clinical trials, being active on different leukemia and solid tumor xenografts (2–4) after oral administration (2, 3).

Although ST1926, CD437, and congeners are bona fide retinoids activating the classic nuclear retinoic acid receptors with different selectivity and potency (3), there are RRMs that do not bind classic nuclear retinoic acid receptors (5, 6). Unlike classic retinoids, RRMs induce apoptosis by undefined intracellular events that eventually unleash the intrinsic and/or extrinsic pathways (1). In myeloma cells (7), nuclear events do not seem to be required for the apoptotic responses, as CD437 acts primarily at the level of the mitochondrion (7), perhaps via relocation of the orphan nuclear receptor, NUR77, from the nucleus (8–10). However, direct targeting of the mitochondrion by RRMs is unlikely. In breast carcinoma cells, the nuclear orphan receptor, Shp/NROB2, binds certain RRMs and plays a major role in the ensuing apoptotic process (11). There is also limited evidence suggesting that ST1926 (12) and possibly CD437 (1, 13, 14) are DNA-damaging agents. However, it is unclear whether DNA damage precedes or is a consequence of the rapid apoptosis triggered by RRMs.

In this report, we use the RRM-sensitive acute myeloid leukemia cell line (NB4) and a derived subline (NB4.437r) selected for induced resistance to RRMs to define the role of

Received 4/30/08; revised 6/19/08; accepted 7/13/08.

Grant support: Associazione Italiana per la Ricerca contro il Cancro, Negri-Weizmann Foundation, Fondo Italiano per la Ricerca di Base progetto internazionalizzazione project RBIN049E44 (E. Garattini), Fondazione Italo Monzino, and Sigma-Tau (Istituto di Ricerche Farmacologiche ''Mario Negri'').

The costs of publication of this article were defrayed in part by the payment of page charges. This article must therefore be hereby marked *advertisement* in accordance with 18 U.S.C. Section 1734 solely to indicate this fact.

Note: C. Valli and G. Paroni equally contributed to the work.

Requests for reprints: Enrico Garattini, Laboratory of Molecular Biology, Department of Biochemistry and Molecular Pharmacology, Istituto di Ricerche Farmacologiche ''Mario Negri,'' via La Masa 19, 20157 Milan, Italy. Phone: 39-2-39014533; Fax: 39-2-39014744. E-mail: egarattini@marionegri.it

doi:10.1158/1535-7163.MCT-08-0419

DNA damage (2, 15, 16). Our results support the notion that ST1926, CD437, and analogues cause phase-specific DNA double-strand breaks (DSB). DSBs are observed only in the sensitive subline, precede apoptosis, and are likely to be responsible for cell demise. The general significance of RRM-induced DSBs for the apoptotic process is confirmed on a panel of other AML cell lines.

Materials and Methods

Chemicals and Cell Culture

ST1926, CD437, and all the other RRMs were synthesized as described (17). Other chemicals used were H_2O_2 (Merck), doxorubicin (Sigma), z-VAD-fmk (Alexis), the DNA-dependent protein kinase (DNA-PK) inhibitor 2-hydroxy-4-morpholin-4-yl-benzaldehyde or IC60211 (Merck), the ataxia telangectasia mutated (ATM) inhibitor 2-morpholin-4-yl-6-thianthren-1-yl-pyran-4-one or KU55933 (Merck), etoposide (Alexis), aphidicolin (Sigma). U937, HL-60, Kasumi-1 (18), the NB4 and the RRM-resistant NB4.437r AML cell lines, and freshly isolated blasts from the peripheral blood of an AML patient were grown in RPMI 1640 containing 10% fetal bovine serum (2). The DNA-PK deficient V3-3 Chinese hamster ovary (CHO) cell line is defective in nonhomologous end joining (NHEJ) and was used with the parental counterpart, CXR3 (19). The parental V79, the homologous recombination (HR)-deficient and Brca2-deficient V-C8, and the complemented V-C8-bac cell lines have been described (20). All CHO cell lines were cultured in Ham's F-10 containing 10% fetal bovine serum (21).

Fluorescence-Activated Cell Sorting, Immunofluorescence, and Western Blot Analyses

Cell cycle analysis was done after staining with propidium iodide (PI; Sigma), using fluorescence-activated cell sorting (FACS; FACSCalibur; Becton Dickinson; ref. 15). Determination of H2AX phosphorylation by FACS analysis was conducted with anti-γ-H2AX and Alexa 488-labeled secondary antibodies (Molecular Probes) on TO-PRO-3-stained cells (20). Flow cytometry studies involving bromodeoxyuridine (BrdUrd) were conducted as detailed (15). Immunofluorescence experiments (22) were done using the following primary antibodies: anti-γ-H2AX (phosphorylated S139; Upstate Biotechnologies) and anti-DNA-PK (phosphorylated T2609; Abcam). Cells were examined with a fluorescence microscope (Olympus BX51) and for high magnification with a laser scan microscope (Leica TCS NT) equipped with a 488 to 534 λ argon laser and a 633 λ He-Ne laser. Western blot analyses were done according to a chemiluminescence-based protocol (GE Healthcare) with anti-γ-H2AX (phosphorylated S139; Upstate Biotechnologies), anti-phosphorylated ataxia telangectasia RAD3-related (ATR; S1981; Rockland), anti-phosphorylated ATM (S428; Cell Signaling), anti-phosphorylated p38 (T180/Y182; Cell Signaling), anti-p38 (Cell Signaling), anti-phosphorylated p53 (S15; ref. 23), and anti-p53 (Santa Cruz Biotechnologies). Secondary anti-rabbit, anti-mouse, and anti-goat horseradish peroxidase-conjugated antibodies were purchased from Sigma.

Colony Assays, Alkaline COMET Assays, and Chromosome Aberrations

Colony assays using V3-3, CXR3, V-C8, V79, and V-C8bac cells were done following treatment with vehicle or increasing concentrations of ST1926 for 4 h (24). The cellular (CACA) and subcellular (SACA) variants of the alkaline COMET assays were done as described (25) and according to Kasamatsu et al. (26), respectively. For each sample, 100 cells or nuclei were acquired using a Zeiss fluorescence microscope connected to an Ultrak CCD black-and-white camera. The statistical calculations of the percent tail DNA were carried out using the Kinetic Comet 5.0 software from Kinetic Imaging. Chromosome aberration analysis was done using exponentially growing NB4wt and NB4.437r cells (27).

Results

ST1926 and CD437 Arrest the Growth of NB4 Cells and Induce Cytotoxicity during S Phase

The growth and viability of NB4 cells is reduced dose-dependently after challenge for 24 h with the RRMs, ST1926, ST2718, and CD437 (Fig. 1A). The three molecules exert a mixed cytotoxic and cytostatic effect, with the former predominating at high concentrations and the latter at low concentrations (<0.2 μmol/L). NB4.437r cells are resistant to ST1926, ST2718, and CD437, with resistance indexes (NB4.437r EC_{50}/NB4 EC_{50}) of 245, 38, and 62, respectively. NB4 and NB4.437r cells are equally sensitive to direct and indirect DNA-damaging agents like ionizing radiations, UV-C light, the topoisomerase inhibitors, camptothecin and etoposide, the ATM inhibitor, the DNA-PK inhibitor, and the histone deacetylase inhibitor SAHA (Supplementary Fig. S1)[7] as well as other chemotherapeutic agents (16).

To study growth inhibition and cytotoxicity separately, exponentially growing NB4 blasts were treated with ST1926 or CD437 (0.1 and 1.0 μmol/L) for up to 48 h. A concentration of ST1926 (0.1 μmol/L) associated with an almost pure cytostatic effect causes a delay in the growth of NB4 cells, which is evident until 24 h (Fig. 1B). At the same concentration, CD437 is devoid of any significant antiproliferative action. When exposed to a predominantly cytotoxic concentration of ST1926 or CD437 (1 μmol/L), NB4 cells undergo rapid apoptosis (15, 16), which is followed by diminished viability.

Alterations in the cell cycle of NB4 cells were evaluated by FACS analysis after staining with PI. DNA histogram profiles after treatment with vehicle, ST1926, or CD437 for 12 and 24 h (Fig. 1C, *left*), as well as a summary of the quantitative results obtained at all the time points (Fig. 1C, *right*) are illustrated. After 12 and 24 h, the majority of NB4 cells treated with 0.1 μmol/L ST1926 shows a delay in the S phase of the cycle. In line with growth recovery (Fig. 1B),

[7] Supplementary material for this article is available at Molecular Cancer Therapeutics Online (http://mct.aacrjournals.org/).

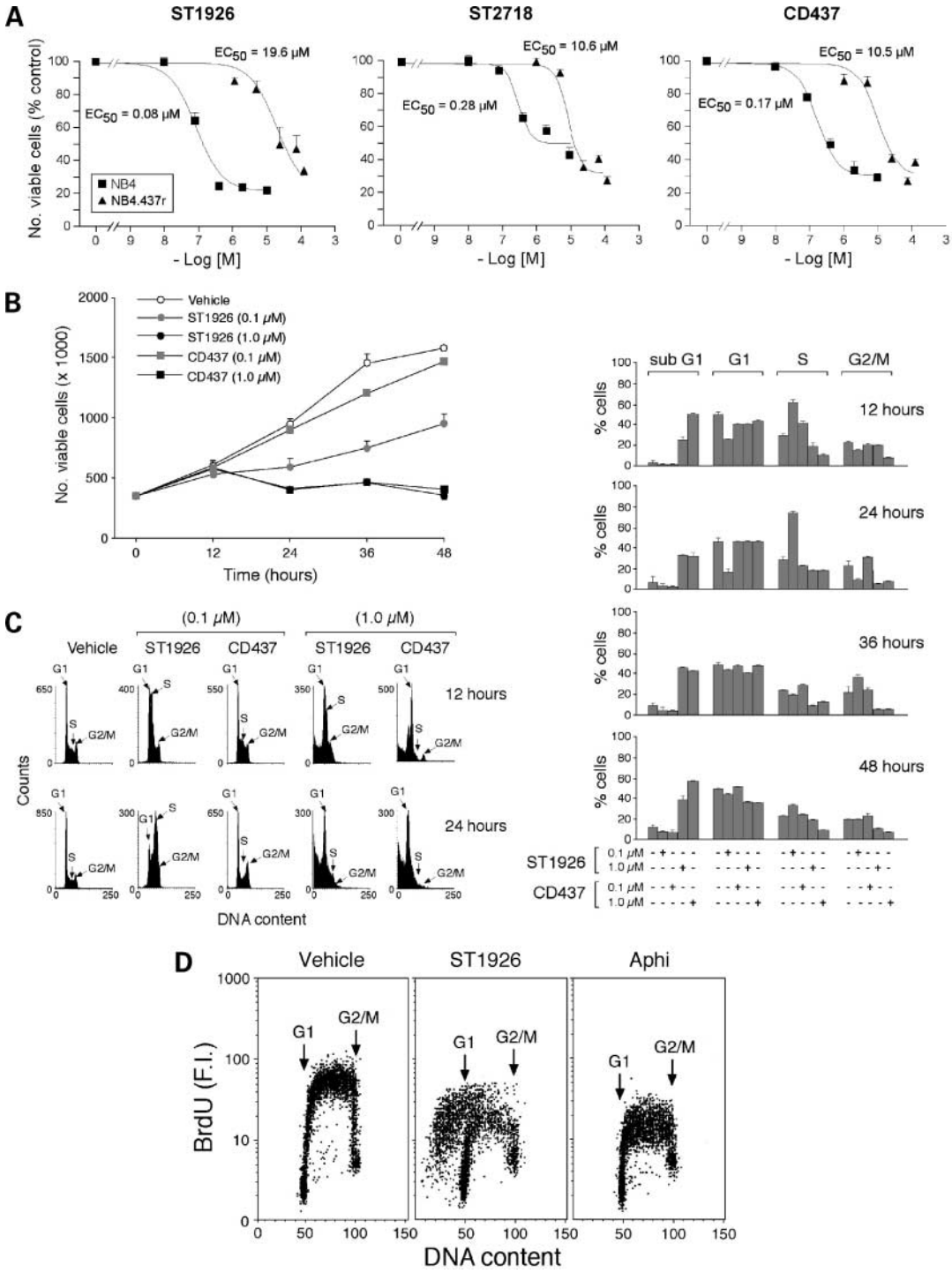

Figure 1. Effects of low and high doses of RRMs on the growth and survival of NB4 and NB4.437r cells: specific action on the S phase of the cell cycle. **A,** NB4 and NB4.437r cells (350,000/mL) were treated with the indicated concentrations of ST1926, CD437, and ST2718 for 24 h. The number of viable cells was determined after staining with trypan blue. Mean ± SD of three replicate cultures. The concentration necessary to decrease by 50% the number of viable cells (EC_{50}) is indicated close to each curve. Representative of at least two independent experiments. **B,** NB4 cells (350,000/mL) were treated for different lengths of time with vehicle (DMSO) or the indicated concentrations of each compound. The number of viable cells was determined after staining with trypan blue. Mean ± SD of three replicate cultures. **C,** representative FACS analyses of NB4 cells (350,000/mL) treated with vehicle or the indicated compound and stained with PI (*bottom left*). *Right,* results obtained after quantification of FACS plots similar to those illustrated in *left*. Mean ± SD of two replicate cultures. Representative of two independent experiments. **D,** NB4 cells (500,000/mL) were coincubated with BrdUrd (10 μmol/L) and vehicle (DMSO), ST1926 (1 μmol/L), or aphidicolin (3 μmol/L) for 3 h. Cells were harvested and stained with FITC-labeled anti-BrdUrd antibodies as well as PI before FACS analysis. The position of cells in the G_1 and G_2-M phase of the cycle is shown. Representative of three independent experiments.

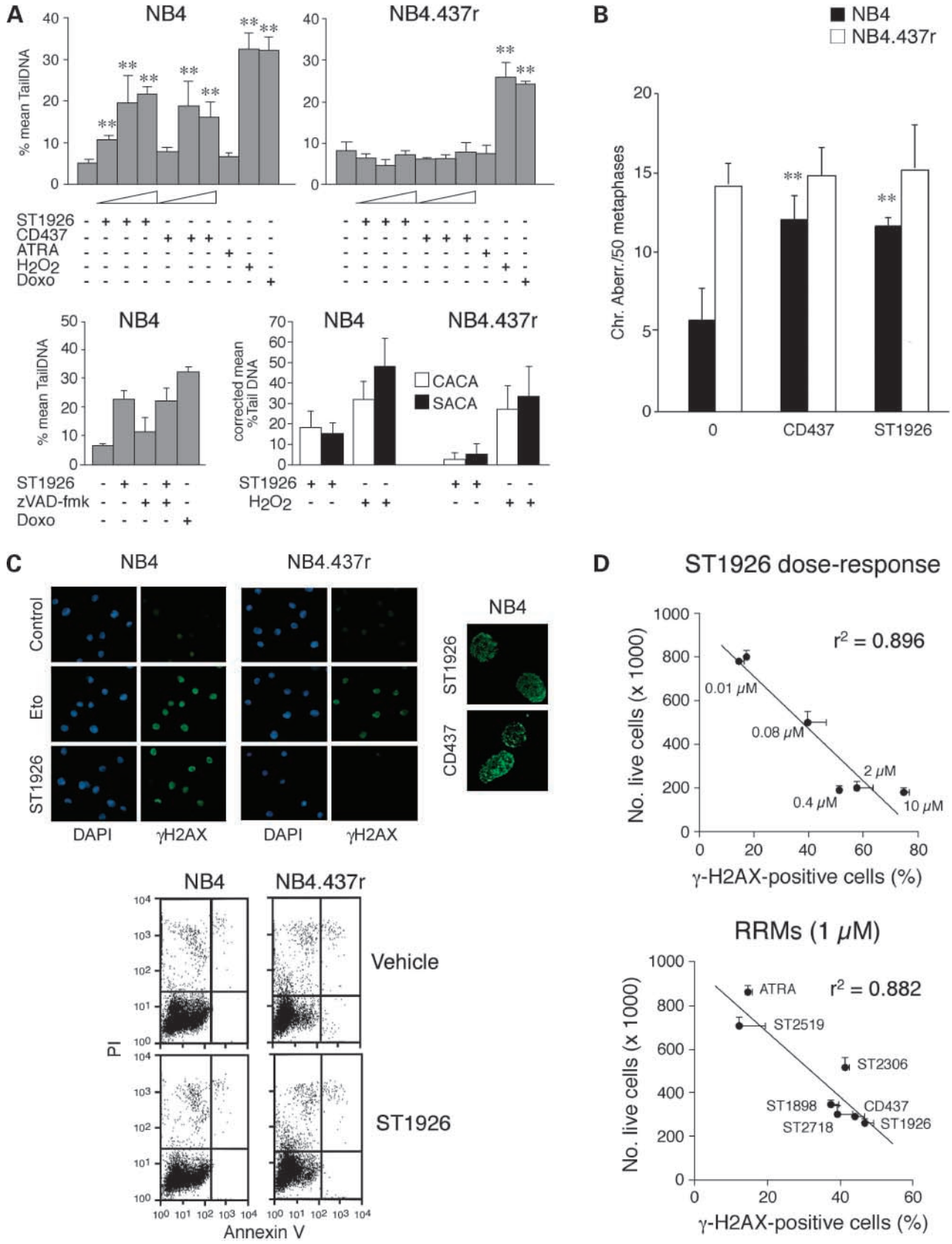

the situation tends to normalize at 36 and 48 h, where no significant difference in the cell cycle distribution of control and ST1926-treated cells is observed (Fig. 1C, *right*). Similarly, 0.1 μmol/L CD437 increases the percentage of NB4 cells in S phase. However, relative to ST1926, the effect is weaker and less protracted, being evident only at 12 h. At 24 h, treatment with 1 μmol/L ST1926 or CD437 results in a selective depletion of the NB4 blasts in the S and G_2-M phase. This is accompanied by the appearance of cells with a sub-G_1 content of DNA at all the time points considered. Once again, NB4.437r blasts are totally refractory to ST1926 and CD437 even in terms of alterations in the cell cycle profile (data not shown). Altogether, our results indicate that growth-inhibitory and noncytotoxic concentrations of ST1926 and CD437 exert their effects predominantly during the S phase (28). Likewise, NB4 cells engaged in DNA synthesis are preferential targets for ST1926 and CD437 used at cytotoxic concentrations.

To establish the role of DNA synthesis and replication in the cytotoxic action of RRMs, we cotreated NB4 cells with BrdUrd and 1 μmol/L ST1926 for 3 h (Fig. 1D). After RRM treatment, the vast majority of the cells showing a sub-G_1 DNA content are also BrdUrd positive, supporting the concept that actively replicating blasts are the primary target of the cytotoxicity of RRMs. As a control for this type of experiments, we used the cytostatic agent, aphidicolin, which causes simple inhibition of DNA replication (decrease in BrdUrd incorporation).

RRMs Induce DSBs in NB4 but Not in NB4.437r Cells: Correlation between DNA Damage and Cytotoxicity

To establish whether RRMs are DNA-damaging agents, CACA was done in NB4 and NB4.437r cells treated with ST1926 or CD437 (Fig. 2A). CACA detects a wide range of DNA lesions, including strand breaks, incomplete excision repair, and alkali-labile sites (29). Treatment of NB4 cells with the two RRMs for 2 h results in a dose-dependent increase in the percentage of cells showing DNA tailing indicative of DNA damage. For both ST1926 and CD437, the effect plateaus between 1 and 2 μmol/L. However, positivity to CACA is observed with 0.1 μmol/L ST1926 but not with the same concentration of CD437. DNA damage is not blocked by preincubation with z-VAD-FMK, an inhibitor of caspases, indicating that the lesions are not secondary to apoptosis. Neither ST1926 nor CD437 induces significant DNA damage in the NB4.437r subline. Resistance is selective, as NB4 and NB4.437r cells are equally sensitive to doxorubicin and H_2O_2. DNA damage in NB4 cells treated with ST1926 does not require the presence of intact cells, as it is visible also with isolated nuclei. Indeed, similar levels of DNA lesions are observed using CACA or SACA (26). In NB4.437r cells, the determinants of the resistance to DNA damage must equally reside in the nuclear fraction. Indeed, SACA (Fig. 2A, *bottom right*) shows that NB4.437r nuclei do not show DNA lesions after challenge with concentrations of ST1926 damaging the DNA of NB4 nuclei.

We determined whether RRMs are capable of inducing chromosomal aberrations in NB4 or NB4.437r cells (Fig. 2B), as these are often observed if DNA damage is triggered during cell replication (30). Incubation of NB4 cells with both ST1926 and CD437 (1 μmol/L) generates an increase in the number of metaphase aberrations. Relative to the NB4 counterpart, NB4.437r cells have higher basal levels of chromosomal aberrations, suggesting augmented genomic instability. In the RRM-resistant cell line, neither ST1926 nor CD437 exerts any further cytogenetic damage. Notably, most of the chromosomal aberrations induced in NB4 cells are of the chromatid type, in line with the concept that the two RRMs require cells to transit along the S phase to induce DNA lesions (30).

Determination of γ-H2AX is the golden standard for DNA DSBs (31). Hence, the presence of nuclear foci containing the phosphorylated form of histone H2AX was evaluated in NB4 and NB4.437r cells (Fig. 2C). Treatment of NB4 but

Figure 2. Active RRMs induce DNA damage and chromosomal aberrations before any sign of apoptosis in NB4 but not in NB4.437r cells: correlation between induction of DSBs and cytotoxicity. **A,** exponentially growing NB4 and NB4.437r cells were subcultured in 24-well plates at 3×10^4 per well the day before drug treatment. Cells were treated for 2 h with ST1926 or CD437 at 0.1, 1, and 2 μmol/L. Vehicle- and ATRA-treated cells (1 μmol/L, 2 h) were used as negative controls, whereas H_2O_2-treated (50 μmol/L, 5 min on ice) and doxorubicin-treated (5 μmol/L, 2 h) samples were run as positive controls for DNA damage. Cells were subjected to standard COMET assays (CACA) done under alkaline conditions. *Top,* results are expressed as the percentage of cells showing signs of DNA damage (tailed cells expressed as % tail DNA). Mean of four replicate cultures. *Bottom left,* CACA of NB4 cells treated in the same conditions as in **A** with or without pretreatment in the presence of the caspase inhibitor z-VAD-FMK (20 μmol/L, 30 min preincubation followed by 2 h coincubation with the drugs). Mean ± SD of three replicate cultures. *Bottom right,* a comparison of the results obtained with CACA and SACA. In the case of CACA, NB4 and NB4.437r cells were treated for 1 h with vehicle (DMSO), ST1926 (2 μmol/L), or H_2O_2 (50 μmol/L) for 5 min at 4°C, and COMET assays were done as above. In the case of SACA, nuclei isolated from NB4 and NB4.437r cells (26) were incubated with DMSO or ST1926 for 2 h or H_2O_2 (50 μmol/L) for 5 min at 4°C. Data were expressed by subtracting the average total % tail DNA of the control cells from the average total % tail DNA of the treated cells. Mean ± SD of three replicate preparations. Representative of three independent experiments. **, $P < 0.01$, statistically higher than the relative controls (Student's *t* test). **B,** induction of chromosomal aberrations in NB4 and NB4.437r cells. Cells (300,000/mL) were treated with 1 μmol/L CD437 or ST1926 for 6 h. In the last 3 h of treatment, 5×10^{-6} mol/L colchicine was added to the medium. Chromosome aberrations (chromatid breaks = S-phase-dependent) were scored in 50 metaphases in repeated experiments. Gaps were not included in the total rate. Mean ± SD of three replicate cultures. Representative of two independent experiments. **, $P < 0.01$, statistically higher than the relative controls (Student's *t* test). **C,** NB4 or NB4.437r cells (400,000/mL) treated with 1 μmol/L ST1926, 1 μmol/L CD437, or 5 μmol/L etoposide for 1 h were stained with 4′,6-diamidino-2-phenylindole to visualize nuclei or with antibodies directed against the phosphorylated form of the histone (γ-H2AX). Results were obtained by confocal microscopy (indirect fluorescence with a FITC-conjugated secondary antibody) at two different magnifications. Representative of at least three independent experiments. *Bottom,* FACS analyses of NB4 and NB4.437r cells after treatment with DMSO (vehicle) or ST1926 (1 μmol/L) for 1 h. Cells were stained with FITC-labeled Annexin V, an early marker of apoptosis, and PI for the DNA content. **D,** *top,* NB4 cells were treated with the indicated concentrations of ST1926, and H2AX phosphorylation (1 h) along with cytotoxicity (18 h) were determined. *Bottom,* NB4 cells were treated with the indicated RRM or ATRA (1 μmol/L), and H2AX phosphorylation (1 h) along with cytotoxicity (24 h) were determined. Mean ± SD ($n = 3$). *Right,* highly significant r^2 correlation values.

not NB4.437r cells with ST1926 and CD437 for 1 h is associated with the appearance of γ-H2AX-positive foci in the nucleus. Lack of γ-H2AX positivity in RRM-treated NB4.437r blasts is not due to deficits in the DNA damage response. In fact, NB4 and NB4.437r cells, which are equally sensitive to etoposide cytotoxicity (data not shown), respond to the topoisomerase II inhibitor with the formation of an equivalent number of γ-H2AX-positive foci. DSBs precede and are not the consequence of apoptosis. Indeed, positivity of γ-H2AX in NB4 cells treated with ST1926 (1 μmol/L) for 1 h is not associated with the appearance of an early apoptotic marker like Annexin V binding activity. In our standard culture conditions, NB4 blasts become positive to Annexin V only after 2.5/3 h of treatment with 1 μmol/L ST1926 or CD437 (data not shown), whereas NB4.437r blasts remain negative indefinitely.

Quantitative correlations between DNA damage and RRM-induced cytotoxicity were sought for by measuring the levels of γ-H2AX after treatment of NB4 cells with RRMs for 30 min (see Fig. 3A for representative results) and the number of viable cells after 24 h (Fig. 2D). There is a linear correlation between histone H2AX phosphorylation and cytotoxic activity, when various concentrations of ST1926 are used. In NB4.437r cells, ST1926 is unable to cause significant H2AX phosphorylation (Supplementary Fig. S2),[7] even at high and cytotoxic concentrations (19 μmol/L), suggesting that high doses of the RRM overcome resistance via activation of alternative mechanisms unrelated to the generation of DSBs. This is apparently at variance with what observed in a recently developed lung carcinoma cell line made resistant to ST1926 (12), suggesting differences in the mechanisms underlying selective RRM resistance in the two cellular models. Indeed, the DNA damage deficit in the RRM-resistant pulmonary cell line may be secondary to a defect in the apoptotic response causing deficient caspase-dependent DNA fragmentation.

To extend the correlation between DNA damage and cytotoxicity to other members of the RRM family, CD437, ST1926, and congeners (the chemical structure of the compounds is present in Supplementary Fig. S3)[7] were used to measure H2AX phosphorylation and antileukemia activity in NB4 cells with test compounds at 1 μmol/L. Once again, a direct relationship between the two variables is evident for all the molecules considered, whereas all-*trans* retinoic acid (ATRA), used as a control, is devoid of DNA damaging activity (Fig. 2D).

S Phase Is a Preferential Target of RRM-Induced DNA Damage

Histone H2AX phosphorylation during the various phases of the cell cycle was studied in NB4 and NB4.437r cells by FACS analysis (Fig. 3A). When treated with ST1926 (1 μmol/L, 30 min), NB4 cells transiting through the S phase of the cycle have higher levels of H2AX phosphorylation than the corresponding counterparts in G_1 or G_2-M. Increased phosphorylation over what observed in control conditions is already evident in S-phase NB4 cells after 15 min of treatment with ST1926. At the same time point, a similar background level of phosphorylated histone is observed in G_1 and G_2-M cells. No significant H2AX phosphorylation is induced by ST1926 in NB4.437r cells regardless of the cycle phase.

We extended the studies on DNA damage/cytotoxicity and cell cycle specificity to other AML cells (Fig. 3B). U937, HL-60, and Kasumi-1 myeloid cells arrest their growth and die in a dose-dependent fashion when challenged with ST1926 or CD437. With the two highest RRM concentrations, growth arrest and cytotoxicity of U937 and HL-60 (but not Kasumi-1) blasts (24 h) are preceded by typical apoptosis (6 h). After 1 h of treatment with 1 or 10 μmol/L ST1926 or CD437, maximal phosphorylation of H2AX in U937 and Kasumi-1 cells is observed during S phase. A similar effect is evident in the other RRM-responsive AML cell line, KG1 (data not shown). In HL-60 cells, the effect is more complex as S-phase selectivity is observed only at low concentrations of the two RRMs. Taken together, our data indicate that DNA damage and consequent early induction of H2AX phosphorylation after treatment with RRMs is a general phenomenon in replicating AML cells.

When maintained in standard conditions, primary cultures of AML blasts are often arrested in the G_0-G_1 phase (Fig. 4A). Relative to control conditions, treatment with ST1926 or CD437 (1 μmol/L) even for prolonged periods of time is not associated with a significant reduction in the number of cells and their viability. By the same token, treatment with ST1926 or CD437 for 30 min or 24 h does not increase H2AX phosphorylation. These results were confirmed in two other AML patients (data not shown) and indicate refractoriness of growth-arrested blasts to RRM-induced DNA damage (γ-H2AX negativity after 1 h of treatment with 1 μmol/L ST1926) and cytotoxicity (no difference in the level of cell viability after 48 h of continuous exposure to 1 μmol/L ST1926).

ATRA causes arrest of NB4 and many other cell types in G_1 (32). Hence, we evaluated whether pretreatment with noncytotoxic concentrations of ATRA affects the response of NB4 cells to ST1926 or CD437 (Fig. 4B). ATRA causes a marked contraction of the S phase after 4 days of treatment. Relative to vehicle pretreatment, cells pretreated with ATRA show a 2-fold increase in viable cells after challenge with ST1926 or CD437 for 24 h. A similar effect is observed in NB4 cells treated with etoposide. As expected, challenge of vehicle pretreated NB4 cells with the two RRMs for 1 h is associated with increased H2AX phosphorylation, which is not evident after pretreatment with ATRA, although long exposures to this last compound augment background levels of the phosphorylated protein. This further supports the concept that RRM-induced DNA damage and cytotoxicity are S-phase specific and suggests that combinations between classic and atypical retinoids should be considered with caution.

RRM Induced DNA Damage Precedes Inhibition of DNA Replication

In the case of certain antitumor drugs, DNA replication plays an active role in the generation of DSBs (33). Thus, we compared the effect of ST1926, aphidicolin, and etoposide

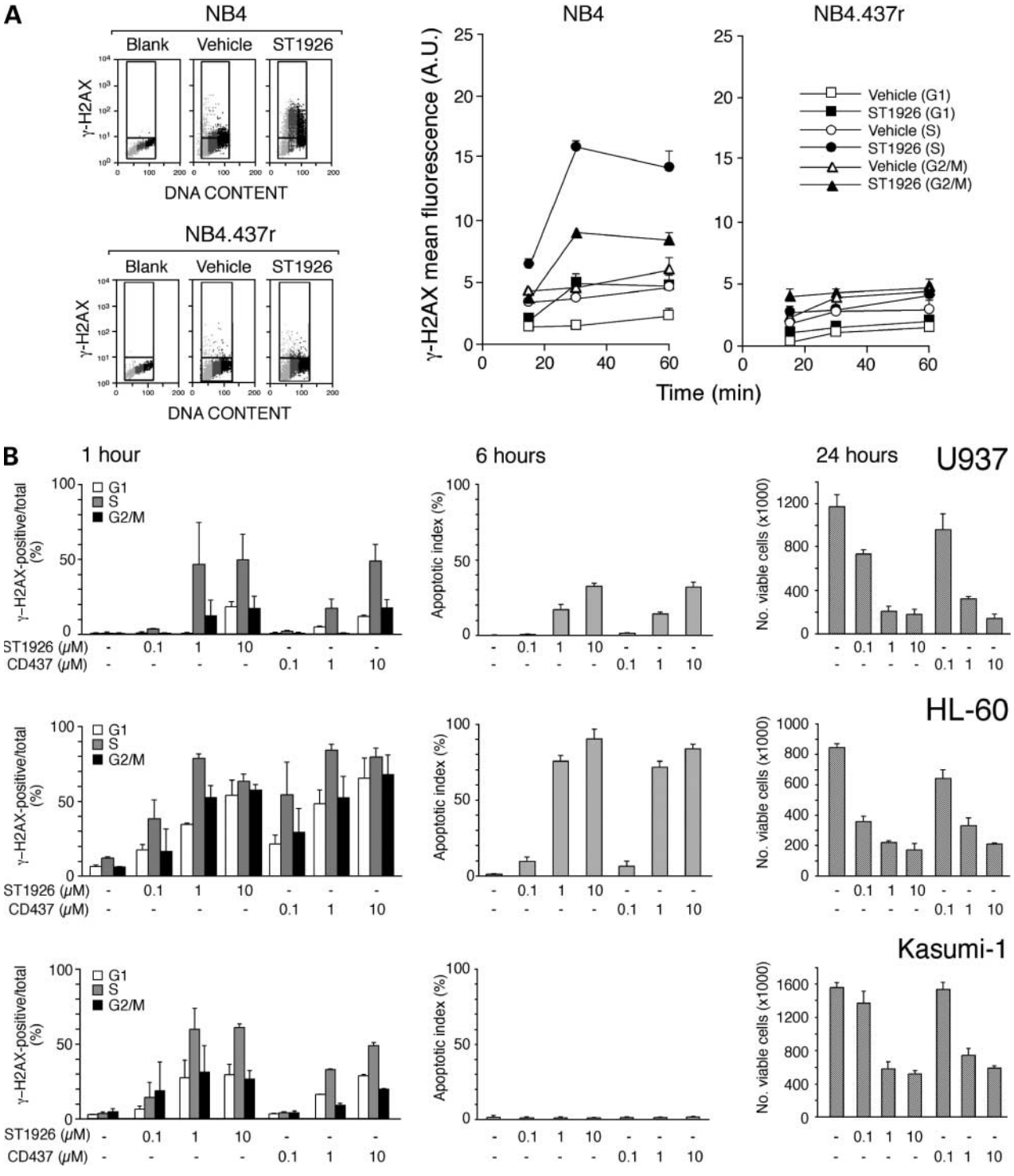

Figure 3. S-phase selectivity of RRM-induced DNA damage in AML cell lines. **A,** NB4 or NB4.437r cells (400,000/mL) were treated for 30 min with ST1926 (1 μmol/L). *Left,* representative FACS analysis of cells after staining for phosphorylated H2AX and PI (DNA content). The events obtained in the G_1, S, and G_2-M phases of the cell cycle are represented by *light gray, dark gray*, and *black dots*, respectively. *Middle* and *right,* time course of the quantitative results obtained in NB4 and NB4.437r cells subjected to the same FACS analyses illustrated in the *left*. Mean ± SD of two replicate cultures. **B,** U937 (*top*), HL-60 (*middle*), and Kasumi-1 (*bottom*) cells seeded at 400,000/mL were treated with the indicated concentrations of ST1926 or CD437 for variable lengths of time. After 1 h (*left*), 6 h (*middle*), and 24 h (*right*) of treatment, aliquots of the cultures were subjected to FACS analysis as in **A**, counted for the number of apoptotic nuclei after staining with 4′,6-diamidino-2-phenylindole, and scored for the number of viable cells after staining with trypan blue, respectively. Data relating to H2AX phosphorylation are expressed as the ratio of γ-H2AX-positive cells to the total number of cells in the corresponding phase of the cycle. Mean ± SD (n = 3).

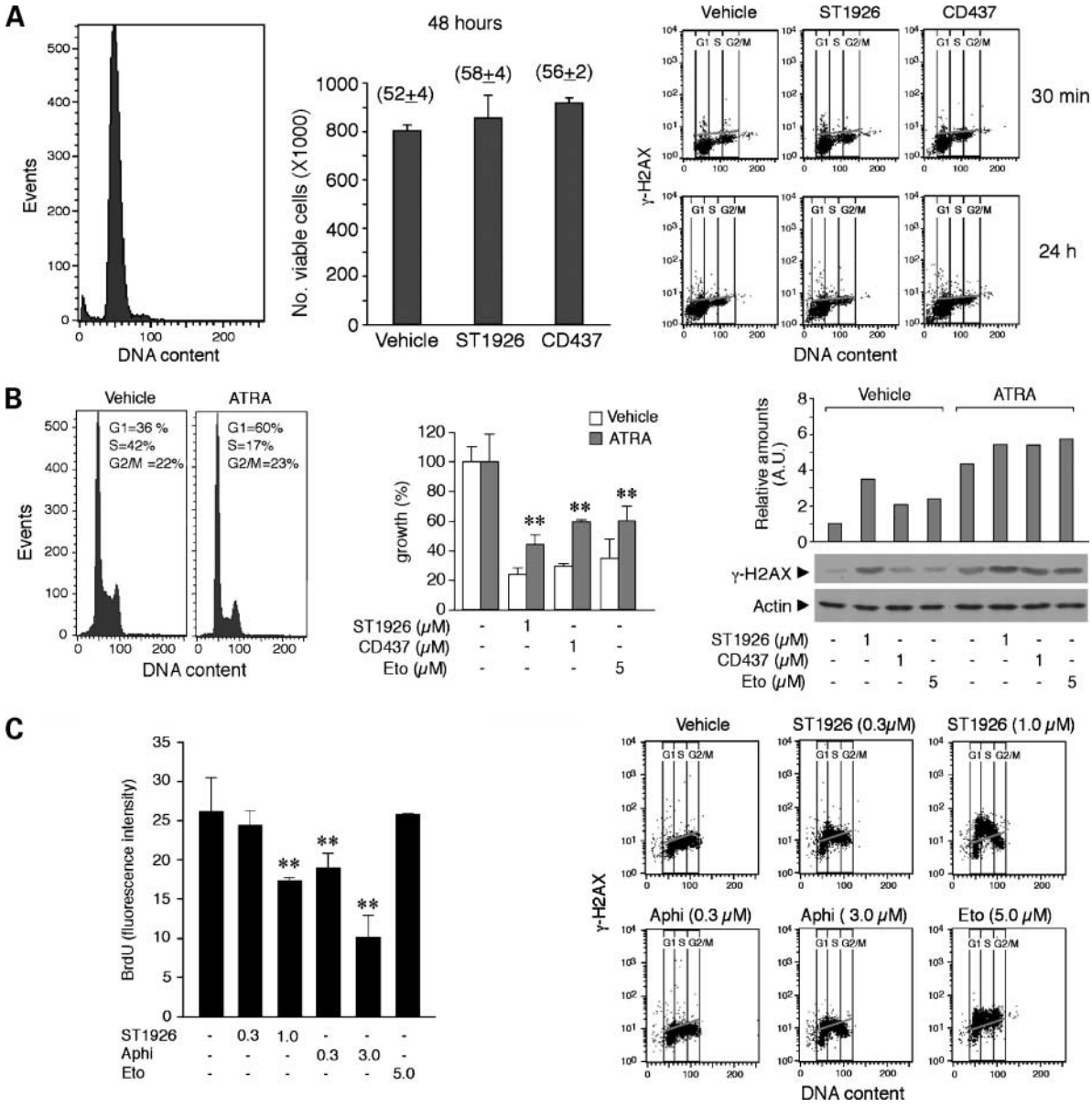

Figure 4. Effects of ST1926 and CD437 in replicating or nonreplicating AML cells: RRMs induce DNA damage before inhibition of replication. **A,** blasts of a representative AML patient (M1 according to the French-American-British classification; 2×10^6 cells/mL) were isolated from the bone marrow and cultured in RPMI 1640 containing 10% fetal bovine serum in the absence or presence of RRMs (1 μmol/L) for the indicated amount of time. *Left,* PI staining of the cells at the beginning of the experiments indicates that all the cells are arrested in G_0. *Middle,* number of viable cells after staining with trypan blue. The viability of cells at the end of the experiment is indicated in parentheses. Mean ± SD of three replicate cultures. *Right,* after staining with PI and anti-phosphorylated H2AX antibodies (indirect fluorescence with a FITC-conjugated secondary antibody), cells were fixed and subjected to FACS analysis. *X axis,* PI-associated fluorescence (DNA content); *Y axis,* phosphorylated H2AX-associated fluorescence. The majority of cells is H2AX negative, indicating lack of DNA damage. Similar results were obtained with blasts from two other AML patients. **B,** NB4 cells (100,000/mL) were pretreated with vehicle or ATRA for 4 d. At the end of the pretreatment, cells were subjected to FACS analysis after PI staining (*left*). The histogram indicates an enrichment in the G_1 phase of the cell cycle in ATRA-pretreated cells. At the end of the pretreatment phase, cells challenged with vehicle or ATRA were diluted in drug-free medium at the same density (400,000/mL) and treated for a further 24 h with the indicated concentrations of ST1926, CD437, or etoposide and the number of viable cells counted (*middle*). Results are expressed as the percentage of viable cells persisting in drug-treated relative to vehicle-treated cultures. Mean ± SD ($n = 3$). **, $P < 0.01$, significantly higher than the corresponding experimental group pretreated with vehicle (Student's *t* test). An aliquot of the cells collected 1 h after drug addition was subjected to Western blot analysis for the quantitative determination of H2AX phosphorylation (*right*). The histogram shows the results obtained after densitometric analysis of the blot. Data are normalized for the actin signal. Representative of two independent experiments. **C,** NB4 cells (500,000/mL) were incubated with BrdUrd (10 μmol/L) in the presence of vehicle or the indicated concentrations of ST1926, aphidicolin, and etoposide for 30 min. An aliquot of the cells was subject to FACS analysis after staining with anti-BrdUrd antibodies. The histogram indicates the amount of BrdUrd associated with cells determined by measuring mean fluorescence intensity. Mean ± SD ($n = 3$). **, $P < 0.01$, significantly lower than the vehicle-treated (*leftmost column*) experimental group (Student's *t* test). Samples obtained as described above were subjected to FACS analysis for the determination of H2AX phosphorylation (*right*). Each FACS plot is representative of two replicate cultures showing identical results.

on the incorporation of BrdUrd (Fig. 4C). ST1926 (0.3 μmol/L) does not alter this variable when NB4 cells are cotreated with the RRM and the nucleotide analog for 30 min. When ST1926 is used at 1 μmol/L, a reduction in the amount of incorporated BrdUrd is observed. Two concentrations (0.3 and 3 μmol/L) of aphidicolin, causing a purely antiproliferative effect and used as controls, determine a much stronger inhibition of BrdUrd incorporation than the RRM. In contrast, a concentration of etoposide (5 μmol/L) equivalent to 1 μmol/L ST1926 in terms of growth inhibition and cytotoxicity (data not shown) is devoid of any effect on DNA replication. The data obtained with 0.3 μmol/L ST1926 indicate that the RRM induces H2AX phosphorylation without affecting BrdUrd incorporation, consistent with the view that DSBs precede inhibition of DNA replication.

ST1926 Activates Kinases Involved in H2AX Phosphorylation and DNA Repair

ATM (34, 35), ATR (34, 36, 37), and DNA-PK represent major sensors of DNA damage and activate H2AX phosphorylation directly or indirectly (35, 38).

Challenge of NB4 but not NB4.437r cells with ST1926 (1 μmol/L) causes rapid (15 min) and persistent phosphorylation/activation of ATM (Fig. 5A). Unlike ATM, maximal ATR phosphorylation is transient and observed after 15 and 30 min (Fig. 5B). This is followed by a return to background phosphorylation levels within 2 h. Phosphorylation/activation of DNA-PK was followed by immunofluorescence (Fig. 5B). Foci containing phosphorylated DNA-PK are evident in the nuclei of NB4 cells after 30 min of treatment with ST1926 and CD437 (1 μmol/L). The foci persist for up to 2 h (data not shown). DNA-PK-positive foci are not present in NB4.437r cells subjected to the same treatment with ST1926 as the parental counterparts. In contrast, RRM-dependent DNA-PK phosphorylation is readily activated in both NB4 and NB4.437r cells challenged with etoposide and aphidicolin. Phosphorylation/activation of ATM, ATR, and DNA-PK is accompanied by phosphorylation of the downstream target, p53, in NB4 but not in NB4.437r cells (Fig. 5A). Phosphorylation of p53 is already detectable at 15 min and evident at 2 h. Based on the phosphorylation kinetics, we cannot differentiate among ATM, DNA-PK, or ATR as the kinases involved in this phosphorylation event. Furthermore, it remains to be established whether phosphorylation of p53 on S15 is followed by acetylation, as the two post-translational modifications are linked and cause activation of the protein (39).

We evaluated whether ATM and/or DNA-PK are involved in ST1926-dependent phosphorylation of histone H2AX, pretreating NB4 cells with the specific inhibitors, IC60211 and KU55933 (Fig. 5C). Inhibition of either ATM or DNA-PK dampens ST1926-dependent H2AX phosphorylation, indicating that both kinases contribute to the post-translational modification of the histone. As expected (40), only the ATM inhibitor suppresses the phosphorylation of histone H2AX triggered by etoposide (5 μmol/L).

CD437 and ST1926 are known to activate mitogen-activated protein kinases, and p38 has been implicated in RRM-induced apoptosis (16). Furthermore, p38 is involved in the DNA repair response (41) and in the formation of γ-H2AX foci (42). Hence, we defined the kinetics of p38 activation by ST1926 in NB4 and NB4.437.r cells (Fig. 5D). In NB4 cells, increased ST1926-dependent phosphorylation of p38 is evident after 2 h and remains elevated until 6 h. Treatment of NB4.437r cells with ST1926 (1 μmol/L) does not result in the phosphorylation/activation of p38. Comparison of the phosphorylation kinetics of p38, ATM, ATR, and DNA-PK indicates that activation of the mitogen-activated protein kinase is a late event, which is subsequent to the formation of γ-H2AX foci. In accordance with this, pharmacologic inhibition of p38 has no effect on the cytotoxic activity of RRMs (2).

Low Levels of DSBs Induced by RRMs Are Repaired: Role of Homologous Recombination

To establish whether DSBs induced by ST1926 and congeners are repaired, we treated NB4 cells with low doses of ST1926 (0.3 μmol/L) for 1 h, washed the drug out, and determined the levels of H2AX phosphorylation (Fig. 6A). In these experimental conditions, the RRM causes a transitory delay in the growth of NB4 cells lasting 24 h. ST1926 induces a rapid increase in the levels of H2AX phosphorylation, evident soon after resuspension in drug-free medium and persisting for at least 1 h. Once again, most of H2AX phosphorylation is associated with S-phase cells. Phosphorylation is reduced dramatically by 16 h and has returned to background levels by 24 h. Hence, DNA damage can be repaired before functional recovery of NB4 cells, although the process is slow and requires at least 24 h to be complete.

HR and NHEJ are the most important DSB repair processes. Whereas HR is operative predominantly during DNA replication, NHEJ is active throughout the cell cycle (43, 44). We compared the sensitivity of NHEJ- or HR-deficient CHO mutant cells and the corresponding normal or genetically complemented counterparts (Fig. 6B). Treatment of the parental (CXR3) or the DNA-PK and NHEJ-deficient V3-3 cell line with ST1926 causes a dose-dependent decrease in the number of colonies scored after replating in drug-free medium. The EC_{50} values are not different in the two cell lines, suggesting that NHEJ is not involved in the repair of ST1926-induced DSBs. In contrast, HR is a major determinant for the repair of RRM-induced DNA damage. Indeed, the BRCA2-deficient VC8 cell line is almost 100-fold more sensitive to the cytotoxic insult caused by ST1926 than the normal V79 counterpart. Partial rescue is observed in VC8 cells stably transfected with a bacterial artificial chromosome (VC8-bac) carrying a DNA fragment containing the BRCA1 and BRCA2 genes. Increased sensitivity of the VC8 cell to ST1926 is associated with higher and more persistent H2AX phosphorylation compared with the V79 counterpart (Fig. 6C). After treatment with ST1926 for 4 h, the level of H2AX phosphorylation is high in the VC8 cells, although it is not different from background in the V79 counterparts.

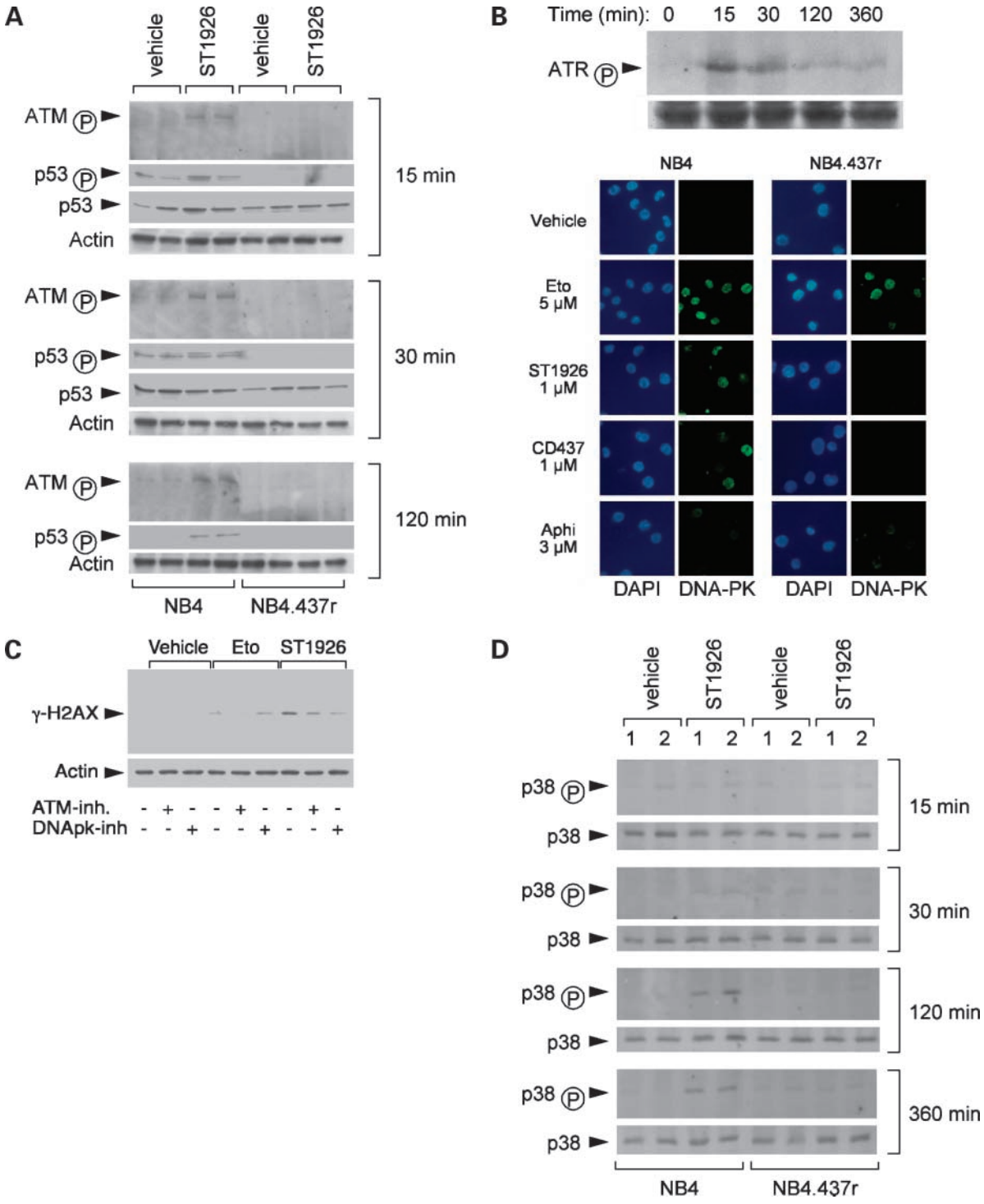

Figure 5. Activation of DNA repair-related phosphatidylinositol kinases and p38 by RRMs: role in H2AX phosphorylation. **A** and **B,** NB4 and NB4.437 cells (300,000/mL) were treated with 1 μmol/L ST1926, 1 μmol/L CD437, 5 μmol/L etoposide, and 3 μmol/L aphidicolin for the indicated amount of time. Cell extracts were subjected to Western blot analysis for the determination of phosphorylated ATM, ATR, and p53 using specific antibodies. In the case of DNA-PK cells, indirect immunofluorescence studies were done to visualize the protein. DNA-PK-containing nuclear foci are shown in cells counterstained with 4′,6-diamidino-2-phenylindole. **C,** NB4 cells were pretreated with vehicle (DMSO) or the indicated ATM and DNA-PK inhibitors for 1 h. This was followed by 1 h treatment with vehicle (DMSO), 1 μmol/L ST1926, or 5 μmol/L etoposide for a further 1 h. Cell extracts were subjected to Western blot analysis for the determination of phosphorylated H2AX or actin. Representative of three independent experiments. **D,** NB4 and NB4.437 cells (300,000/mL) were treated with vehicle (DMSO) or 1 μmol/L ST1926 for the indicated amount of time. Cell extracts were subjected to Western blot analysis for the determination of phosphorylated p38, total p38, or actin.

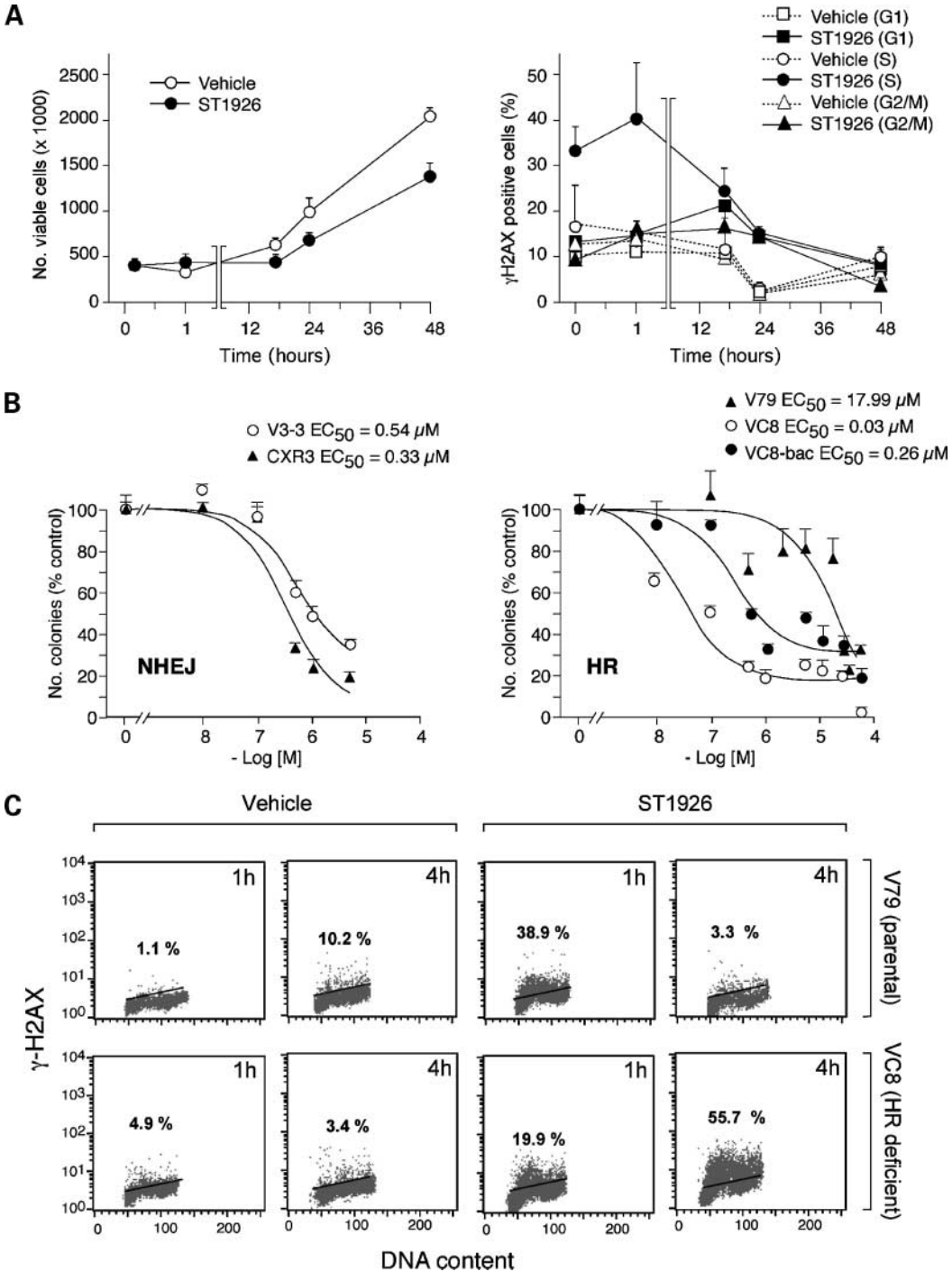

Figure 6. Significance of HR for the repair of ST1926-induced DNA damage. **A,** NB4 cells were treated for 1 h with vehicle (DMSO) or ST1926 (0.3 μmol/L). At the end of the treatment (time 0), cells were washed and resuspended in drug-free medium. The number and viability of cells was assessed on an aliquot of the culture after staining with trypan blue (*left*). Mean ± SD of three replicate cultures. Another aliquot of the culture was subjected to FACS analysis after staining for γ-H2AX and TO-PRO-3. *Right,* percentage of γ-H2AX-positive cells in the G_1, S, and G_2-M phases of the cell cycle. Mean ± SD of two replicate cultures. **B,** parental CXR3 and NHEJ-defective (V3-3, XRCC7-/-) or parental V79, HR-deficient (V-C8, BRCA2$^{-/-}$) and partially complemented VC8-bac (stably transfected with a bacterial artificial chromosome carrying a DNA fragment containing the BRCA1 and BRCA2 genes) CHO cells were treated with the indicated concentrations of ST1926 for 4 h. Crystal violet-positive cell colonies were counted after 5 d. Results are expressed as the percentage of control cultures. Mean ± SD (n = 3). Representative of three independent experiments producing identical results. **C,** HR-deficient VC8 and parental V79 cells were treated with vehicle (DMSO) or ST1926 (1 μmol/L) for the indicated amount of time and subjected to FACS analysis after staining for γ-H2AX and PI. The percentage of γ-H2AX-positive cells is indicated. Each panel is representative of duplicate cell cultures showing superimposable results.

Selective accumulation of ST1926-dependent DSBs in the HR-deficient cells is evident despite initial lower induction of γ-H2AX at 1 h, consistent with ineffective repair.

Discussion

This report provides evidence that RRMs are DNA-damaging agents, producing DSBs (45), particularly during the S phase of the cell cycle. In the case of ST1926, DSBs are observed with concentrations of the drug (≥0.2 μmol/L), which are clinically achievable. Indeed, phase I clinical trials indicate that oral administration of the drug at intermediate dose levels (200 mg/d) results in peak plasma concentrations around 1 μmol/L.[8] In NB4 cells, there is a direct quantitative correlation between the levels of DSBs and the cytotoxic/antiproliferative effects caused by ST1926, CD437, and congeners. RRM-resistant NB4.437r cells do not show DNA damage after treatment with RRMs. These and similar results obtained with U937, HL-60, Kasumi-1, and KG1 cells indicate that RRM-induced DNA damage is at the basis of the antiproliferative and apoptotic response observed in AML cells. In addition, the correlation between DNA-damaging and cytotoxic activity within the chemical series of ST1926 analogues suggests that the same functional groups dictating cytotoxicity are also responsible for genotoxicity in NB4 cells. Induction of DSBs by active RRMs is a very early phenomenon observed minutes after treatment and is not secondary to apoptosis. Following short exposure to low concentrations of RRMs, DSBs can be repaired and HR seems to be the main mechanism underlying the repair process. Based on the experiments conducted in NHEJ-deficient and nucleotide excision repair-deficient CHO cells (Fig. 6B; Supplementary Fig. S4),[7] these other modalities do not seem to be relevant for the repair of RRM-induced lesions.

The nature and the molecular mechanisms responsible for the DNA damage caused by RRMs are unknown. In particular, it is unclear whether RRMs exert a direct or an indirect genotoxic action. There is evidence that tiny amounts of DNA adducts can be detected in cells exposed to apoptotic concentrations of CD437 (13, 14). We observed that DNA covalent binding of CD437 is 3-fold higher in NB4 than in NB4.437r cells after exposure to the radioactive compound (1). Because the chemical structure of the adducts is unknown, it is possible that they are the result of intrinsic chemical reactivity of CD437 toward DNA or the consequence of enzymatic activation to short-lived reactive metabolites by undefined systems, such as cytochrome *P*450-dependent monooxygenases (46, 47). Although the presence of ST1926-derived adducts have not yet been shown, the data obtained with CACA and SACA are against the idea of DNA-damaging reactive metabolites, as similar levels of DNA lesions are observed after exposure of intact cells and isolated nuclei. Indeed, as nuclei are largely devoid of cytochrome *P*450-dependent activity (48), our results are more consistent with DNA damage being the consequence of effects triggered by the intact ST1926 molecule. Notably, pretreatment of NB4 cells with two cytochrome *P*450-dependent inhibitors, like metyrapone and SKF525A, does not affect the antileukemic activity of ST1926 and CD437.[9] Given the S-phase specificity of RRMs, it is possible that DNA adducts cause replication-dependent induction of DSBs if the advancing replication fork stalls or collapses. However, this is unlikely, because BrdUrd incorporation experiments indicate that generation of DSBs precedes inhibition of DNA replication.

Beside the formation of DNA adducts, there are several other possible causes for RRM-induced DSBs. Generation of clastogenic oxygen radicals by CD437 has been shown in HL-60 cells after 30 min of treatment (49). These reactive species could be generated via uncoupling of the mitochondrial redox chain potentially induced by the immediate and long-standing elevation of intracellular calcium triggered by RRMs (2). However, we could not show increased production of oxygen radicals in RRM-treated NB4 cells using fluorescent probes like dichlorofluorescein and dihydroethidine.[10] Furthermore, pretreatment of cells with the free radical scavenger, *N*-acetylcysteine, does not protect NB4 cells from ST1926-induced cytotoxicity and DNA damage.[10] Inhibition of specific components of the DNA synthesis or repair machineries may also induce DSBs. Experiments involving BrdUrd incorporation are against the first possibility, because generation of DSBs occurs before inhibition of DNA replication. Selective inhibition by ST1926 or CD437 of a crucial component of the HR system can also be excluded, as deficit of the DNA repair process is indeed associated with an increase in RRM-induced DNA damage. In contrast, the possibility that RRMs inhibit NHEJ and nucleotide excision repair cannot be dismissed, as the two types of CHO deficient cells used may have alterations in molecules that are not targeted by RRMs.

An important point emanating from our study regards the relationship, if any, between RRM-induced DNA damage and intracellular calcium mobilization, as this last phenomenon is also of significance for RRM-dependent cytotoxicity (2). Potential links between the two phenomena are at the level of DNA repair, as multiple steps in the process are calcium dependent (50). Alterations in the homeostatic balance of intracellular calcium triggered by RRMs may impair specific steps of the various DNA repair pathways, causing DSBs and trigger apoptosis. Ongoing studies in our laboratory are aimed at addressing this and related issues.

Definition of the determinants responsible for the selective resistance of NB4.437r cells may shed light on the molecular mechanisms of the antileukemic activity of RRMs. Resistance to RRMs is not due to differences in the

[8] C. Pisano, unpublished results.

[9] Unpublished results.

[10] C. Valli and G. Paroni, unpublished observations.

accumulation of ST1926 inside NB4 and NB4.437r blasts (Supplementary Fig. S5).[7] Furthermore, NB4.437r cells do not show deficits in the DNA damage or general responses to UV and ionizing radiations. Instead, our results show that resistance of the NB4.437r cell line to RRMs is associated with refractoriness to induced DSBs and subsequent activation of damage sensors like ATM, ATR, DNA-PK, and p38 activation. SACA shows that the molecular determinants of RRM resistance reside in the nucleus. Lack of DSBs in NB4.437r cells could result from increased DNA repair or decreased DNA damage. Increased DNA repair is unlikely, as DSBs are observed in NB4 but not in NB4.437r cells even after very short exposures (3 min; data not shown) to high concentrations of ST1926. Decreased DNA damage may be primary or secondary to deficiency/structural alteration of DNA repair components inhibited by RRMs. Whole-genome transcriptome analysis of NB4 and NB4.437r cells[11] suggest alterations in chromatin structure. The absence of DSBs in NB4.437r cells may be due to a more compact chromatin causing reduced accessibility of RRMs to DNA or other nuclear targets. Quantitative or qualitative alterations of a DNA repair component bound and inhibited by RRMs provide another explanation for the lack of H2AX phosphorylation observed in NB4.437r cells. Nevertheless, the data obtained with etoposide and specific inhibitors of ATM and DNA-PK indicate that these putative RRM targets cannot be ATM, ATR, DNA-PK, or histone H2AX themselves.

In conclusion, our study indicates that phase-specific DNA damage is an important determinant of RRM-induced antileukemic activity. RRMs seem to induce DNA lesions via mechanisms that are different from those of other DNA-damaging agents. This suggests that RRMs may be used in combination with other genotoxic chemotherapeutics, such as cisplatin (4). Studies addressing this point are in progress in our laboratory. It also remains to be established whether DNA damage is the major mechanism underlying RRM cytotoxicity in cell types other than replicating AML blasts. Indeed, generalization of our results to solid tumors known to be responsive to RRMs, such as breast and lung carcinoma, is currently unwarranted, as notable differences in the timing, type (cytotoxic versus antiproliferative), and extent of antineoplastic activity in different cellular models are known (1). Nevertheless, our data are relevant in the context of a more rational design of clinical studies aimed at establishing the potential of ST1926 in the management of AML.

Disclosure of Potential Conflicts of Interest

The authors declare no conflict of interest. Dr. Claudio Pisano is a full-time employee of Sigma-Tau Industrie Farmaceutiche Riunite SPA, which holds the patent of ST1926.

[11] E. Garattini and M. Fratelli, unpublished results.

Acknowledgments

We thank Dr. Renzo Bagnati for the measurement of ST1926 in NB4 and NB4.437r cells by liquid chromatography/mass spectrometry, Dr. Hadassa Degani (Weizmann Institute of Sciences) for the useful scientific suggestions and for the collaboration during the course of the study, Dr. Paolo Carminati (Sigma-Tau Industrie Riunite) for critical reading of the article.

References

1. Garattini E, Gianni M, Terao M. Retinoid related molecules an emerging class of apoptotic agents with promising therapeutic potential in oncology: pharmacological activity and mechanisms of action. Curr Pharm Des 2004;10:433 – 48.

2. Garattini E, Parrella E, Diomede L, et al. ST1926, a novel and orally active retinoid-related molecule inducing apoptosis in myeloid leukemia cells: modulation of intracellular calcium homeostasis. Blood 2004;103:194 – 207.

3. Parrella E, Gianni M, Fratelli M, et al. Antitumor activity of the retinoid-related molecules (*E*)-3-(4′-hydroxy-3′-adamantylbiphenyl-4-yl)acrylic acid (ST1926) and 6-[3-(1-adamantyl)-4-hydroxyphenyl]-2-naphthalene carboxylic acid (CD437) in F9 teratocarcinoma: role of retinoic acid receptor γ and retinoid-independent pathways. Mol Pharmacol 2006;70:909 – 24.

4. Pisano C, Vesci L, Fodera R, et al. Antitumor activity of the combination of synthetic retinoid ST1926 and cisplatin in ovarian carcinoma models. Ann Oncol 2007;18:1500 – 5.

5. Farhana L, Dawson MI, Fontana JA. Apoptosis induction by a novel retinoid-related molecule requires nuclear factor-κB activation. Cancer Res 2005;65:4909 – 17.

6. Zhang Y, Dawson MI, Ning Y, et al. Induction of apoptosis in retinoid-refractory acute myelogenous leukemia by a novel AHPN analog. Blood 2003;102:3743 – 52.

7. Marchetti P, Zamzami N, Joseph B, et al. The novel retinoid 6-[3-(1-adamantyl)-4-hydroxyphenyl]-2-naphtalene carboxylic acid can trigger apoptosis through a mitochondrial pathway independent of the nucleus. Cancer Res 1999;59:6257 – 66.

8. Liang B, Song X, Liu G, et al. Involvement of TR3/Nur77 translocation to the endoplasmic reticulum in ER stress-induced apoptosis. Exp Cell Res 2007;313:2833 – 44.

9. Zhang XK. Targeting Nur77 translocation. Expert Opin Ther Targets 2007;11:69 – 79.

10. Han YH, Cao X, Lin B, et al. Regulation of Nur77 nuclear export by c-Jun N-terminal kinase and Akt. Oncogene 2006;25:2974 – 86.

11. Farhana L, Dawson MI, Leid M, et al. Adamantyl-substituted retinoid-related molecules bind small heterodimer partner and modulate the Sin3A repressor. Cancer Res 2007;67:318 – 25.

12. Zuco V, Zanchi C, Lanzi C, et al. Development of resistance to the atypical retinoid, ST1926, in the lung carcinoma cell line H460 is associated with reduced formation of DNA strand breaks and a defective DNA damage response. Neoplasia 2005;7:667 – 77.

13. Zhao X, Spanjaard RA. The apoptotic action of the retinoid CD437/AHPN: diverse effects, common basis. J Biomed Sci 2003;10:44 – 9.

14. Zhao X, Demary K, Wong L, et al. Retinoic acid receptor-independent mechanism of apoptosis of melanoma cells by the retinoid CD437 (AHPN). Cell Death Differ 2001;8:878 – 86.

15. Mologni L, Ponzanelli I, Bresciani F, et al. The novel synthetic retinoid 6-[3-adamantyl-4-hydroxyphenyl]-2-naphthalene carboxylic acid (CD437) causes apoptosis in acute promyelocytic leukemia cells through rapid activation of caspases. Blood 1999;93:1045 – 61.

16. Ponzanelli I, Gianni M, Giavazzi R, et al. Isolation and characterization of an acute promyelocytic leukemia cell line selectively resistant to the novel antileukemic and apoptogenic retinoid 6-[3-adamantyl-4-hydroxyphenyl]-2-naphthalene carboxylic acid. Blood 2000;95:2672 – 82.

17. Cincinelli R, Dallavalle S, Nannei R, et al. Synthesis and structure-activity relationships of new antiproliferative and proapoptotic retinoid-related biphenyl-4-yl-acrylic acids. Bioorg Med Chem 2007;15:4863 – 75.

18. Asou H, Tashiro S, Hamamoto K, Otsuji A, Kita K, Kamada N. Establishment of a human acute myeloid leukemia cell line (Kasumi-1) with 8;21 chromosome translocation. Blood 1991;77:2031 – 6.

19. Arnaudeau C, Lundin C, Helleday T. DNA double-strand breaks associated with replication forks are predominantly repaired by homologous recombination involving an exchange mechanism in mammalian cells. J Mol Biol 2001;307:1235 – 45.

20. Tavecchio M, Simone M, Erba E, et al. Role of homologous recombination in trabectedin-induced DNA damage. Eur J Cancer 2008; 44:609 – 18.

21. Kraakman-van der Zwet M, Overkamp WJ, van Lange RE, et al. Brca2 (XRCC11) deficiency results in radioresistant DNA synthesis and a higher frequency of spontaneous deletions. Mol Cell Biol 2002;22:669 – 79.

22. Paroni G, Henderson C, Schneider C, Brancolini C. Caspase-2-induced apoptosis is dependent on caspase-9, but its processing during UV- or tumor necrosis factor-dependent cell death requires caspase-3. J Biol Chem 2001;276:21907 – 15.

23. Shieh SY, Ikeda M, Taya Y, Prives C. DNA damage-induced phosphorylation of p53 alleviates inhibition by MDM2. Cell 1997;91: 325 – 34.

24. Tavecchio M, Natoli C, Ubezio P, Erba E, D'Incalci M. Dynamics of cell cycle phase perturbations by trabectedin (ET-743) in nucleotide excision repair (NER)-deficient and NER-proficient cells, unravelled by a novel mathematical simulation approach. Cell Prolif 2007;40:885 – 904.

25. Di Francesco AM, Meco D, Torella AR, et al. The novel atypical retinoid ST1926 is active in ATRA resistant neuroblastoma cells acting by a different mechanism. Biochem Pharmacol 2007;73:643 – 55.

26. Kasamatsu T, Kohda K, Kawazoe Y. Comparison of chemically induced DNA breakage in cellular and subcellular systems using the comet assay. Mutat Res 1996;369:1 – 6.

27. Tanzanella C, Antoccia A, Spadoni E, et al. Chromosome instability and nibrin protein variants in NBS heterozygotes. Eur J Hum Genet 2003; 11:297 – 303.

28. Zhang Y, Rishi AK, Dawson MI, et al. S-phase arrest and apoptosis induced in normal mammary epithelial cells by a novel retinoid. Cancer Res 2000;60:2025 – 32.

29. Collins AR. The comet assay for DNA damage and repair: principles, applications, and limitations. Mol Biotechnol 2004;26:249 – 61.

30. Natarajan AT. Chromosome aberrations: past, present and future. Mutat Res 2002;504:3 – 16.

31. Xie A, Hartlerode A, Stucki M, et al. Distinct roles of chromatin-associated proteins MDC1 and 53BP1 in mammalian double-strand break repair. Mol Cell 2007;28:1045 – 57.

32. Wang JG, Barsky LW, Davicioni E, et al. Retinoic acid induces leukemia cell G_1 arrest and transition into differentiation by inhibiting cyclin-dependent kinase-activating kinase binding and phosphorylation of PML/RARα. FASEB J 2006;20:2142 – 4.

33. Soares DG, Escargueil AE, Poindessous V, et al. Replication and homologous recombination repair regulate DNA double-strand break formation by the antitumor alkylator ecteinascidin 743. Proc Natl Acad Sci U S A 2007;104:13062 – 7.

34. Stucki M, Jackson SP. γH2AX and MDC1: anchoring the DNA-damage-response machinery to broken chromosomes. DNA Repair (Amst) 2006;5:534 – 43.

35. Abraham RT. Cell cycle checkpoint signaling through the ATM and ATR kinases. Genes Dev 2001;15:2177 – 96.

36. Appella E, Anderson CW. Post-translational modifications and activation of p53 by genotoxic stresses. Eur J Biochem 2001;268: 2764 – 72.

37. Bao S, Tibbetts RS, Brumbaugh KM, et al. ATR/ATM-mediated phosphorylation of human Rad17 is required for genotoxic stress responses. Nature 2001;411:969 – 74.

38. Weterings E, Chen DJ. DNA-dependent protein kinase in nonhomologous end joining: a lock with multiple keys? J Cell Biol 2007;179:183 – 6.

39. Li M, Luo J, Brooks CL, Gu W. Acetylation of p53 inhibits its ubiquitination by Mdm2. J Biol Chem 2002;277:50607 – 11.

40. Hickson I, Zhao Y, Richardson CJ, et al. Identification and characterization of a novel and specific inhibitor of the ataxia-telangiectasia mutated kinase ATM. Cancer Res 2004;64:9152 – 9.

41. Golding SE, Rosenberg E, Neill S, Dent P, Povirk LF, Valerie K. Extracellular signal-related kinase positively regulates ataxia telangiectasia mutated, homologous recombination repair, and the DNA damage response. Cancer Res 2007;67:1046 – 53.

42. Hsiao PW, Chang CC, Liu HF, Tsai CM, Chiu TH, Chao JI. Activation of p38 mitogen-activated protein kinase by celecoxib oppositely regulates survivin and γ-H2AX in human colorectal cancer cells. Toxicol Appl Pharmacol 2007;222:97 – 104.

43. Hendrickson EA. Cell-cycle regulation of mammalian DNA double-strand-break repair. Am J Hum Genet 1997;61:795 – 800.

44. Takata M, Sasaki MS, Sonoda E, et al. Homologous recombination and non-homologous end-joining pathways of DNA double-strand break repair have overlapping roles in the maintenance of chromosomal integrity in vertebrate cells. EMBO J 1998;17:5497 – 508.

45. Fernandez-Capetillo O, Lee A, Nussenzweig M, Nussenzweig A. H2AX: the histone guardian of the genome. DNA Repair (Amst) 2004;3: 959 – 67.

46. Dechant KL, Brogden RN, Pilkington T, Faulds D. Ifosfamide/mesna. A review of its antineoplastic activity, pharmacokinetic properties and therapeutic efficacy in cancer. Drugs 1991;42:428 – 67.

47. Baird WM, Hooven LA, Mahadevan B. Carcinogenic polycyclic aromatic hydrocarbon-DNA adducts and mechanism of action. Environ Mol Mutagen 2005;45:106 – 14.

48. Garattini E, Gazzotti G, Salmona M. Is nuclear styrene monooxygenase activity a microsomal artifact? Chem Biol Interact 1980;31:341 – 6.

49. Zang Y, Beard RL, Chandraratna RA, Kang JX. Evidence of a lysosomal pathway for apoptosis induced by the synthetic retinoid CD437 in human leukemia HL-60 cells. Cell Death Differ 2001;8: 477 – 85.

50. Bugreev DV, Mazin AV. Ca^{2+} activates human homologous recombination protein Rad51 by modulating its ATPase activity. Proc Natl Acad Sci U S A 2004;101:9988 – 93.